Available online at www.sciencedirect.com
SCIENCE DIRECT
Journal of Molecular Spectroscopy 238 (2006) 79–90
Journal of MOLECULAR SPECTROSCOPY
www.elsevier.com/locate/jms

Combined analysis of the high sensitivity Fourier transform and ICLAS-VeCSEL absorption spectra of D_2O between 8800 and 9520 cm^{-1}

O.V. Naumenko [a], O. Leshchishina [a], S. Shirin [b], A. Jenouvrier [c], S. Fally [d], A.C. Vandaele [e], E. Bertseva [f], A. Campargue [f,*]

[a] *Laboratory of Molecular Spectroscopy, Institute of Atmospheric Optics, SB, Russian Academy of Science, 1, Akademicheckii av., 634055, Tomsk, Russia*
[b] *Institute of Applied Physics of Russian Academy of Sciences, 46, Uljanova St., 603950, Nizhny Novgorod, Russia*
[c] *Groupe de Spectrométrie Moléculaire et Atmosphérique (associated with CNRS: UMR 6089) Université de Reims, Faculté des Sciences BP 1039 - 51687 Reims Cedex 2, France*
[d] *Service de Chimie Quantique, UniversitéLibre de Bruxelles, CP160/09, 50 Av. F.D.Roosevelt, B-1050, Brussels, Belgium*
[e] *Institut d'Aéronomie Spatiale de Belgique, 3, Av.Circulaire, B-1180 Brussels, Belgium*
[f] *Laboratoire de Spectrométrie Physique (associated with CNRS, UMR 5588), Université Joseph Fourier de Grenoble, B.P. 87, 38402 Saint-Martin-d'Hères Cedex, France*

Received 10 March 2006; in revised form 18 April 2006
Available online 26 April 2006

Abstract

The absorption spectrum of dideuterated water, D_2O, has been recorded between 8800 and 9520 cm^{-1} by intracavity laser absorption spectroscopy (ICLAS) based on a vertical external cavity system emitting laser (VeCSEL) and by high sensitivity Fourier Transform spectroscopy. The combined analysis of the spectra has allowed attributing 1223 transitions to the D_2O species. The spectrum assignment was performed on the basis of the recent results of variational calculations based on an optimized potential energy surface of D_2O. A set of 687 energy levels was derived from transitions assigned to eight upper vibrational states, 577 of them being reported for the first time. A detailed line list has been generated. The line intensities were retrieved mainly from the FTS spectrum and the absolute integrated intensities of the $2v_1 + v_2 + v_3$ and the $v_2 + 3v_3$ bands dominating the spectrum have been determined.

Keywords: FTS; Fourier transform spectroscopy; ICLAS; Intracavity laser absorption spectroscopy; Deuterated water; Rovibrational energy levels

1. Introduction

The absorption spectrum of D_2O above 8100 cm^{-1} has been the subject of a few reports:

- the 9160–9390 cm^{-1} section was recorded and analyzed in 1982 by intracavity laser absorption spectroscopy (ICLAS) with a moderated sensitivity of 10^{-7} cm^{-1} using an Nd glass laser [1].
- the $(v_1 + v_2/2 + v_3) = 3.5$ and 4 polyads near 9300 [2] and 10 300 cm^{-1} [3], respectively, were investigated by Fourier transform spectroscopy (FTS) with a 105 m path length.
- the 5OD region (12 570–12 820 cm^{-1}) was recorded by ICLAS-Ti-Sapphire associated with a FTS detection scheme [4].

The present contribution, devoted to the 8800–9520 cm^{-1} region, corresponds to the full coverage of the $(v_1 + v_2/2 + v_3) = 3.5$ polyad which is the 2nd decade of resonating states (the 1st decade lying in the 7500–8300 cm^{-1} region has been analyzed in Ref. [5]). As just mentioned,

* Corresponding author. Fax: +33 4 76 63 54 95.
E-mail address: Alain.Campargue@ujf-grenoble.fr (A. Campargue).

0022-2852/$ - see front matter © 2006 Published by Elsevier Inc.
doi:10.1016/j.jms.2006.04.015

this polyad was previously investigated [1,2] but the higher sensitivity of the experimental methods presently implemented will provide a much deeper knowledge of this spectral region. The absorption spectrum was recorded in parallel in Reims by Fourier Transform spectroscopy with a 600 m path length and in Grenoble by ICLAS based on vertical external cavity surface emitting lasers (VeCSEL). An equivalent sensitivity corresponding to a detection limit $\alpha_{min} \sim 5 \times 10^{-9}\,cm^{-1}$ was achieved in the two recordings. As discussed below, the combination of the two spectra obtained by different methods proved to be a valuable help in the species and rovibrational assignment process.

An overview of the H_2O, HDO, and D_2O stick spectra in the region of interest is presented in Fig. 1 of Ref. [6]. The D_2O spectrum is dominated by two well separated bands: the $2v_1 + v_2 + v_3$ and the $v_2 + 3v_3$ bands centered at 9050.349 and 9366.313 cm^{-1} respectively. A global comparison of the absorbance in the region shows that (for the pure species), the HDO and D_2O absorbance are on the same order of magnitude while the absorbance of $H_2{}^{16}O$ is much stronger than that of the D_2O and HDO isotopologues below 9000 cm^{-1}.

2. Experimental details

2.1. FTS spectrum

The FTS spectra have been recorded by the Bruxelles–Reims (BR) group and the detail of the experimental set-up has been described elsewhere [7–9]. Briefly, a Bruker IFS 120M Fourier transform spectrometer was coupled to a long multiple reflection absorption cell of 50 m base

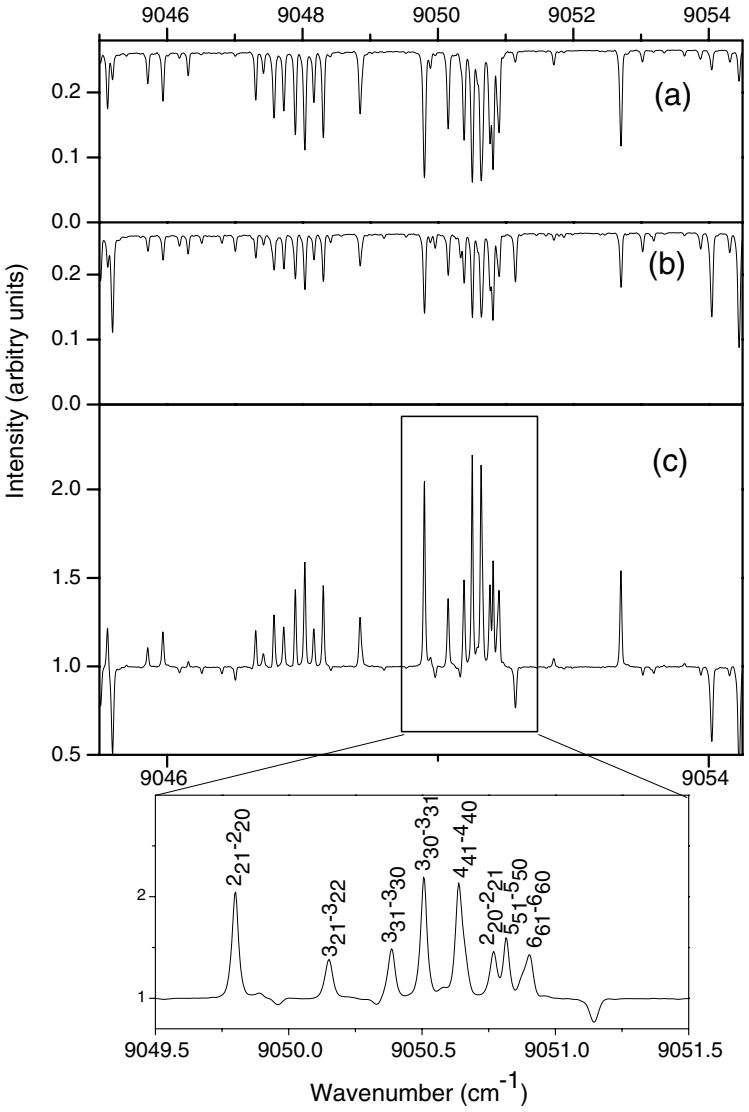

Fig. 1. Illustration of the experimental procedure used to discriminate the D_2O lines among the HDO and H_2O lines in the FTS spectrum by comparison of different spectra recorded with different D_2O/HDO/H_2O mixtures with a 600 m of path length at a resolution of 0.03 cm^{-1}: (a) and (b) correspond to spectrum B, C of Table 1, respectively; (c) presents the ratio C/B of the two spectra. As the D_2O concentration is higher in the B sample than in the C sample, the lines appearing in (c) above the baseline are those of D_2O while the H_2O and HDO lines are observed as absorption lines. This procedure is very efficient to discriminate D_2O transitions. The assignment of the strongest D_2O lines belonging to the $2v_1 + v_2 + v_3$ band is indicated.

length. The unapodized resolution defined as 0.9/maximum optical path difference (Bruker definition) was set to 0.03 cm^{-1}. No apodization function was used. A path length of 600 m was chosen in order to maximize the signal-to-noise (S/N) ratio. The light source was a 250 W tungsten halogen lamp (ORIEL) and the detector was a silicon diode sensitive over the whole spectral range investigated. All the spectra were recorded at room temperature (291 K ± 3 K) monitored in the cell by three platinum resistance thermometers. The temperature was not stabilized and may therefore differ by up to 2 K from one end to the other. Several spectra were recorded successively with a given sample to allow the monitoring of any change in the pressure resulting from condensation on the walls of the cell. Each spectrum was the result of the Fourier transformation of 128 co-added interferograms. To improve the S/N ratio, six spectra corresponding to a total recording time of 15 h, were co-added. A detectivity of $\alpha_{min} \sim 4.5 \times 10^{-9}$ and 2×10^{-8} cm^{-1} corresponding to an rms S/N ratio of 3600 and 800 was achieved at 9500 and 8800 cm^{-1}, respectively.

The $D_2{}^{16}O$ sample was purchased from the Commissariat à l'Energie Atomique (CEA) with a stated purity of 99.9%. In order to discriminate the transitions due to H_2O, HDO or D_2O, different H_2O/D_2O mixtures were introduced into the cell. In these mixtures, the H_2O partial pressure was first determined from the intensity of about one hundred strong and well isolated lines. Then, the HDO and D_2O partial pressures were calculated either by using the equilibrium constant given in [10], $K_{eq} = 3.86 \pm 0.07$ for the reaction $H_2O + D_2O \leftrightarrow 2$ HDO or from the ratios of selected line intensities of the two species. The determined values of the relative $D_2O/HDO/H_2O$ concentrations are reported in percentages in Table 1.

Fig. 1 shows a small section of the absorption spectra B and C (see Table 1) obtained with different experimental conditions. After their wavenumber calibration versus the Hitran 2004 database and the BR database (http://www.ulb.ac.be/cpm/) by using the stronger H_2O lines, the atmospheric contribution due to the absorption within the external path between the light source and the spectrometer was removed by the same procedure as described in Ref. [11]. The D_2O lines were easily identified from the variation of their intensities with the sample composition. The procedure is illustrated on Fig. 1: the D_2O lines are those appearing as peaks on the ratio of spectra B and C.

2.2. ICLAS-VeCSEL spectrum

The ICLAS spectra were recorded with the experimental setup based on a VeCSEL previously described in Refs. [12,13] and recently applied to the study of the HDO absorption spectrum in the same region [6]. The achieved sensitivity was on the order of $\alpha_{min} \sim 5 \times 10^{-9}$ cm^{-1}, which is less than the best performances achieved in other spectral regions (see for instance Refs. [13–16]) as a consequence of the poorer laser properties of the VeCSEL presently used.

The spectra were recorded with generation times up to 130 μs, leading to equivalent absorption path lengths on the order of 23.4 km as the filling ratio of the laser cavity by the absorption cell was 60%. The spectral resolution was about 0.04 cm^{-1} slightly larger than the Döppler broadening (0.028 cm^{-1} FWHM).

As a result of the rapid proton exchange in water and the omnipresence of the main isotopologue, H_2O, adsorbed on the walls of the filling line and of the absorption cell, it is difficult to obtain a sample of water with a largely dominant fraction of the D_2O isotopologue. This was however achieved with the ICLAS cell (about 200 cm^3 volume) as the experimental procedure consisting in successively filling the cell with dideuterated water, recording the spectrum, vacuuming the cell and recording the background spectrum, was performed several hundred of times and then washed out the H_2O isotopologue from the cell. Fig. 2 shows the comparison of the FTS and ICLAS spectra in a spectral section showing only HDO and D_2O lines. The $D_2O/HDO/H_2O$ relative fractions were estimated to be 74/23/3 and 93.7/6.0/0.3 for the FTS and ICLAS samples respectively. The contribution of HDO and H_2O absorption lines was then largely reduced in the ICLAS spectrum which helps to observe D_2O lines when falling in close coincidence with HDO or H_2O transitions.

The ICLAS spectrum was obtained by adding 12 cm^{-1} wide sections of the spectrum recorded successively with the 3754 photodiode array placed at the exit of the spectrograph dispersing the VeCSEL beam. The wavenumber calibration procedure of each elementary spectrum requires the knowledge of reference line positions. We used the HDO line positions measured by FTS [17] as reference which leads to an agreement within about 0.003 cm^{-1} with the line positions measured independently on the FTS spectrum recorded in Reims.

Table 1
Experimental conditions for the FTS spectra recorded in this work

Spectrum	Spectral range (cm^{-1})	Total pressure (hPa)	Relative concentration $D_2O/HDO/H_2O$ (%)	T (K)	Nbr of scans
$H_2O + D_2O$					
A	8500–12000	2.6	56/21/23	293	6 × 128
B	8500–12000	13.3	74/23/3	293	6 × 128
C	8500–12000	13.2	34/50/16	291	6 × 128
Pure H_2O					
D	8500–12000	18.2	0/0/100	291	6 × 128

Note. The path length and resolution for all the spectra were 602.32 m and 0.03 cm^{-1}, respectively.

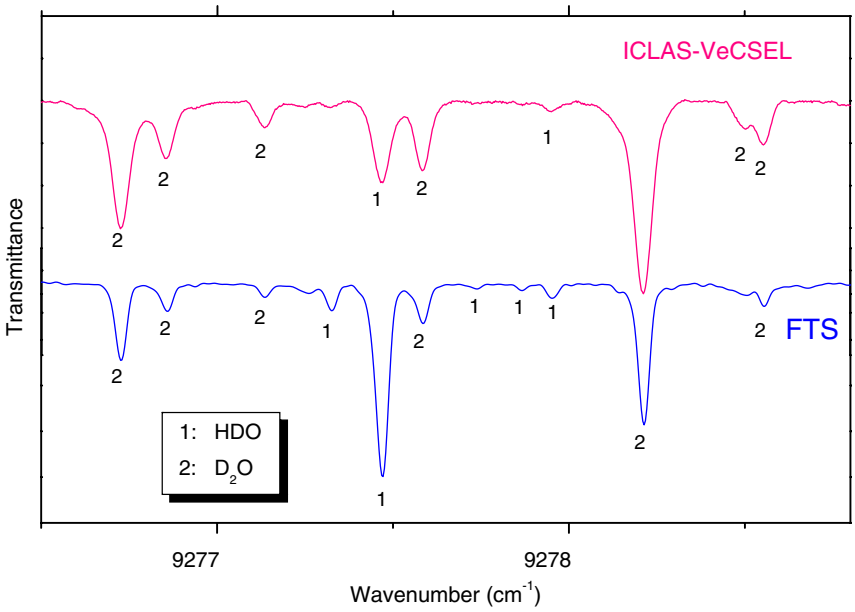

Fig. 2. Comparison of the FTS and the ICLAS-VeCSEL spectra. The experimental conditions (path length, total pressure and sample composition) were the following: FTS (spectrum B): 602.3 m, 13.3 hPa, $D_2O/HDO/H_2O = 74/23/3$ ICLAS: 20.7 km, 23.6 hPa, $D_2O/HDO/H_2O \approx 93.7/6.0/0.3$.

2.3. Line list construction

The D_2O lines were discriminated among the HDO and H_2O lines by using the procedure illustrated in Fig. 2 or using the available H_2O [9,18] and HDO [6] line lists. The D_2O line list between 8800 and 9520 cm^{-1} region was obtained by combining the FTS and ICLAS data in the 9095–9510 cm^{-1} region where the two spectra are available. In this common region, the line positions were found to agree with a 0.004 cm^{-1} rms deviation. The accuracy of the FTS intensities, mainly limited by the uncertainty on the D_2O concentration in the FTS sample is estimated to 10 % for the lines which are not among the weakest. On the other hand, the specific laser dynamics of VeCSELs prevents their use for accurate quantitative measurements by ICLAS-VeCSEL (see Refs. [6,19] for more details about this issue). We then adopted the FTS line intensities for strong and middle intensity lines, which led to a set of 625 FT lines which was gathered with 213, mostly weak, lines measured by ICLAS. As the relative concentration of D_2O compared to H_2O was about 15 times higher in the ICLAS sample compared to the FTS sample with higher D_2O relative concentration (spectrum B), some of the relatively strong lines were also retrieved from the ICLAS spectrum in the case of unrecoverable overlapping with strong H_2O lines Absolute intensities of the ICLAS lines were estimated from their peak absorption and scaled on the FT absolute intensities of the nearby lines. The accuracy of these ICLAS intensities is poorer and estimated to 30–50% on average.

The weakest lines which have been detected have an intensity value on the order of 5×10^{-27} cm/molecule both for FTS and ICLAS.

3. Rovibrational assignment and discussion

3.1. Line assignment

In the assignment process of the resulting set of 1223 D_2O lines, we used the synthetic line list based on D_2O potential energy surface (PES) [20] and Schwenke and Partridge *ab initio* dipole moment surface (DMS) [21]. The D_2O PES was optimized by the fitting to 720 experimental energy levels with the rotational quantum number $J = 0$, 2, 5, and 10. These levels lie up to 13000 cm^{-1} above the ground state. Morphing the original *ab initio* potential energy surface [22] using 25 constants reproduced the levels used in the fit with a standard deviation of 0.033 cm^{-1}. This fit was presently used to generate a line list of all D_2O transitions up to 11 000 cm^{-1} and $J \leqslant 17$. The DVR3D program suite [23] was used with 21 radial grid points for Morse oscillator-like basis functions and 40 angular grid points based on (associated) Legendre polynomials. A final Hamiltonian matrix of dimension 1500 was used for the vibrational calculations and $300 * (J + 1 - p)$ for the rotational calculations, where the parity $p = 0$ or 1. The masses were set at $M_D = 2.013553$ u and $M_O = 15.990526$ u.

In the last years, this assignment procedure based on the comparison of the observed and calculated line parameters has proven to be the most efficient for assigning the water isotopologues spectra. It takes also into account for the regular and smooth tendencies in the deviations of the observed levels from their calculated values. Though the (obs. − calc.) values may reach up to several cm^{-1}, which leads to tens experimental lines as possible candidates for the considered assignment, the existence of evident

(obs. − calc.) tendencies combined with intensity matching still provides reliable assignments.

The deviations for all observed rotational quantum numbers (up to $J = 17$) were found to vary from 0.01 to 0.40 cm^{-1}. We compared our synthetic spectrum [20,21] with that of Partridge and Schwenke [21,24] (PS), which can also be used for D_2O assignment (see, for example, [25,26]). As stated in [25] for low lying vibrational states, the (obs. − calc.) deviations for SP calculation may increase up to 1.2 cm^{-1} but preserve their regular dependence on J and K_a quantum numbers up to J, K_a values around 30 thus providing reliable criteria for assignment of the hot D_2O spectra. However, it is not the case for the spectral region under interest: the (obs. − calc.) deviations for PS calculations loose their regularity and increase much starting at $J = 10$, (see Fig. 3), reaching −1.53 cm^{-1} for $J = 16$. Interestingly, PS HDO synthetic spectrum is much better in the same spectral region, (obs. − calc.) values not exceeding 0.05 cm^{-1} on average [6]. The reason for the poor accuracy of the PS calculations for D_2O may be caused by the fact that, contrary to HDO, the PES of D_2O [24] was not optimized by a fitting to the experimental line positions. In contrast with PS calculations, the presently used D_2O PES which was obtained in Ref. [20], shows though rather large, but regular (obs. − calc.) deviations up to $J = 17$.

For assignment purpose, the intensity and line position matching between theory and experiment are both important. Figs. 4 and 5 illustrate the very satisfactory agreement between the experimental and calculated stick spectra, respectively, in the whole investigated spectral region and in a small interval. The calculated intensities are, on aver-

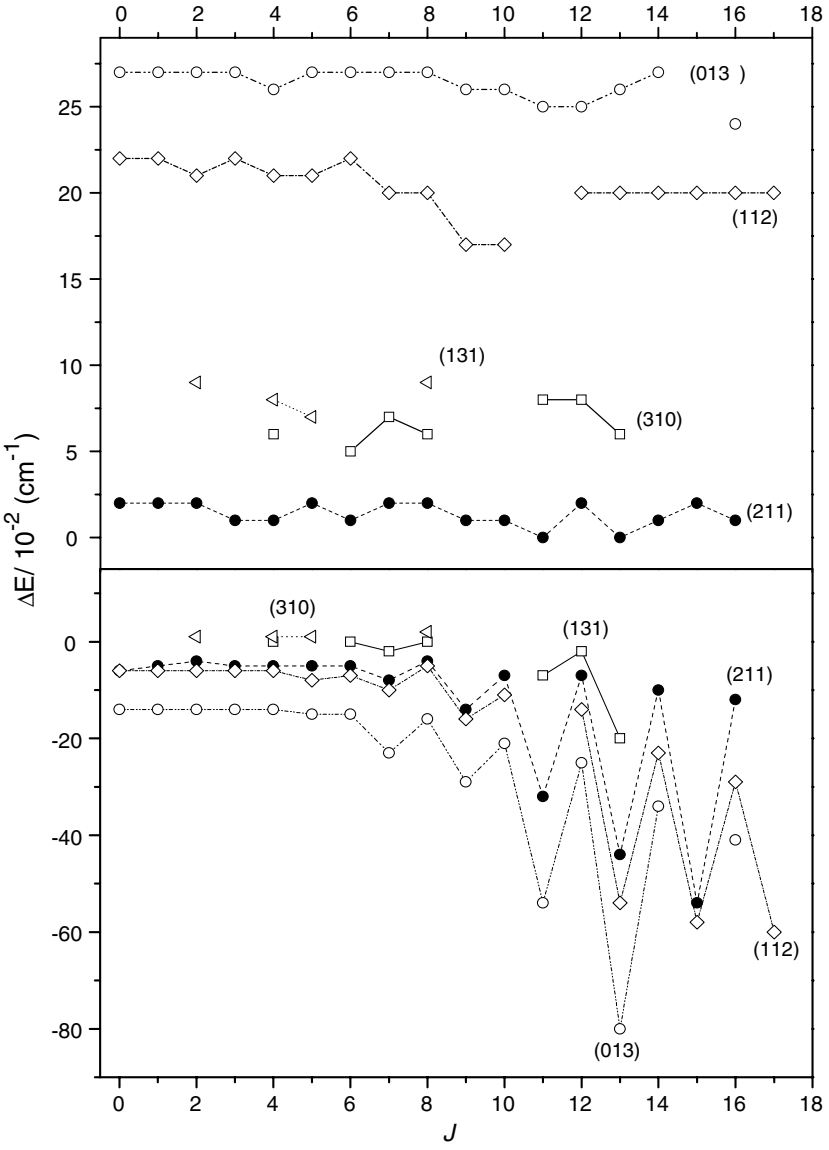

Fig. 3. Plot of the variation of the ($E_{obs.} - E_{calc.}$) differences for the [$J0J$] rotational term values of the analyzed vibrational states. Note the change in the ordinate scale. Upper panel: rotational term values obtained from the D_2O optimized potential energy surface of Ref. [20]. Lower panel: calculated values from Schwenke and Partridge [24].

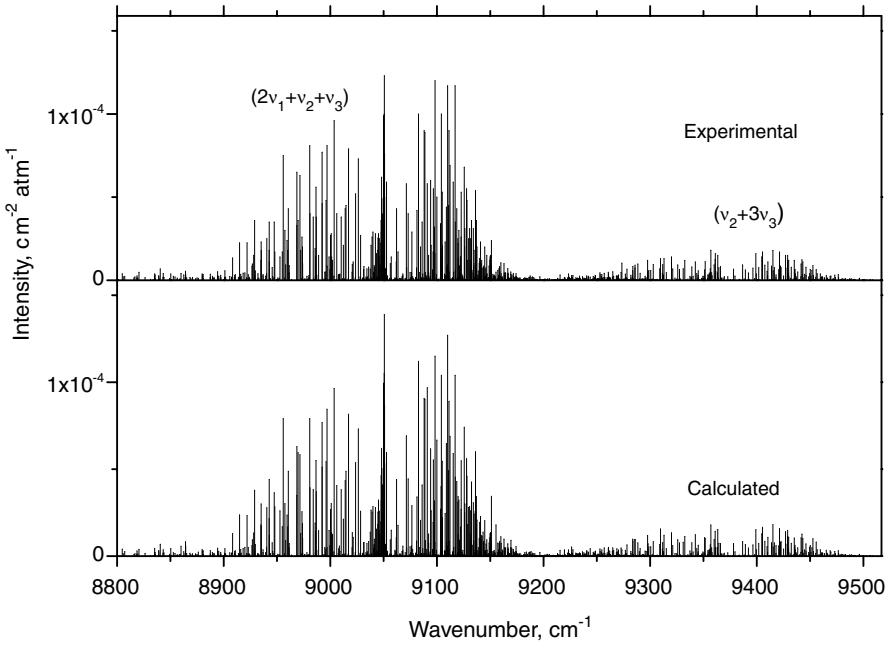

Fig. 4. Comparison of the D_2O stick spectrum between 8800 and 9500 cm^{-1}: upper panel, combined spectrum obtained from FTS and ICLAS recordings (see text); lower panel: synthetic spectrum calculated from the D_2O optimized potential energy surface of Ref. [20] and SP ab initio dipole moment surface [21].

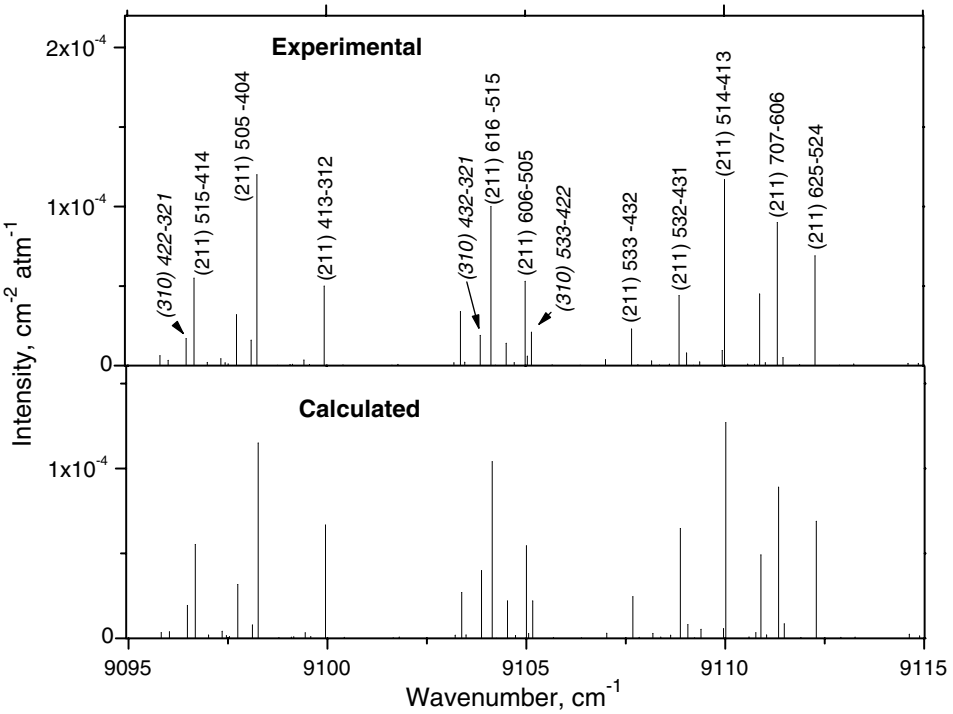

Fig. 5. Same as Fig. 3 for a small spectral section around 9105 cm^{-1}. The $(v_1', v_2', v_3')J'K_a'K_c'$–$J''K_a''K_c''$ rotational assignments are given for part of the lines The spectrum is dominated by transitions of the $2v_1 + v_2 + v_3$ band. A few transitions of the $3v_1 + v_2$ band are also indicated, the whole assignments being listed in the Supplementary Material.

age, strongly dependent on the DMS used, and in much lesser extent on the rovibrational wave functions provided by the PES. Consequently, both sets of calculated intensities considered here coincide very well.

Nearly all (98%) experimental lines attributed to D_2O were assigned. The resulting D_2O line list counting 1430 lines (taking into account unresolved blends) is attached to this paper as Supplementary Material. This list contains

observed positions, observed and calculated [20,21] intensities followed by their rovibrational assignment.

3.2. Energy levels

A summary of the quantitative information obtained in this study is given in Table 2. An important set of 687 accurate energy levels belonging to eight vibrational states listed in Table 2 was derived by adding the ground state experimental rotational energies [26] to the observed transitions. They are listed in Tables 3 and 4. Only separate energy levels were derived for the (032), (230), and (221) states. For the other five states, the number of energy levels is comparable or significantly exceeds that of the main isotopologue, $H_2{}^{16}O$. The band origins for the (131) and (310) states were extrapolated from the (obs. − calc.) tendency for the [*J*0*J*] levels (see Fig. 3). That of the (221) state, presently observed through a hot band, was derived from (221)–(000) transitions assigned in the FTS spectrum between 10000 and 10485 cm^{-1} spectral region.

In our strivings to produce as complete identification of the spectrum as possible, we admit a definite risk of less reliable assignment. The few less reliable assignments as well as the energy levels derived from them are marked as "T" (tentative) in Tables 3 and 4 and in the Supplementary Material. Tentative assignments (16 in total) concern, first of all, single weak lines not included into combination difference relations. They may either significantly deviate from the (obs. − calc.) tendency or from the calculated intensity, or they represent additional assignments to already identified transition. Finally, part of the energy levels is derived from blended lines and has poorer accuracy. These levels are marked by "B" in Tables 3 and 4.

Very weak transitions of the (230)–(000) and (032)–(000) bands seem to borrow their intensities from stronger line-partners belonging to the (310)–(000), (211)–(000) and (131)–(000) bands. In particular, a close resonance with the (211) $K_a = 3$ energy levels yielded a long sequence of experimentally observed transitions involving the (032) $K_a = 4$ upper levels with J varying from 4 to 9. No interpolyad interactions were traced for the 2nd decade of D_2O, indicating that the centrifugal distortion effect in this molecule is weaker than that for other isotopologues like $H_2{}^{16}O$, HDO, $H_2{}^{17}O$, $H_2{}^{18}O$ [27]. However, a number of the (010) energy levels of D_2O with $J > 23$ is perturbed by accidental resonances with higher vibrational states [26].

We included in Table 2 a comparison of the energy levels set presently derived with that of Ref. [2] where a total of 110 levels belonging to the (211), (310), and (032) vibrational states were determined. 103 levels coincide with ours within 0.0021 cm^{-1} while 7 outliers deviate from 0.009 up to 0.034 cm^{-1}. Consequently, the number of newly derived energy levels is 577. The spectrum assignment in [2] was based on the Effective Hamiltonian (EH) approach; seven vibrational states were involved into a simultaneous fit, six of them being, in fact, dark levels. The band origins evaluated in [2] from the energy levels fitting are reproduced in Table 2. Band centers for all dark states excluding (310) deviate from our precise experimental or predicted [20] values by as much as 12.3 cm^{-1}. This situation illustrates one of the most serious drawbacks of the EH method: a poor predictive ability despite the high quality of the fitting.

Despite recent advances in the analysis of the D_2O line positions (see, for example, Refs. [2,4,25,26,28]), much less is known about the D_2O transition intensities. We include in Table 2, the experimental integrated band intensities obtained as the sum of the intensities of all transitions assigned to a given band. (In case of a blended line, the line intensity was attributed to the vibrational level with the dominant contribution). As seen from Table 2, as well as from Fig. 4, the $2v_1 + v_2 + v_3$ band, dominating the 8800–9200 cm^{-1} region, is about seven times stronger than the $v_2 + 3v_3$ band dominating the 9200–9500 cm^{-1} region.

4. Conclusion

High resolution Fourier Transform and ICLAS-VeCSEL spectra of D_2O molecule in the 8800–9520 cm^{-1}

Table 2
Summary of the information obtained from the ICLAS and FT spectra of D_2O recorded between 8800 and 9500 cm^{-1}

Band	Upper state vibrational term value[a] (cm^{-1})			Band intensity (cm/molecule)	J_{max}	$K_{a\,max}$	N levels
	Calc. Ref. [20]	Observed	Ref. [2]				
(230)–(000)	8712.00		8713.31	6.9E−25	10	6	11
(131)–(000)	8792.55	8792.63[b]	8788.60	5.5E−24	13	9	81
(032)–(000)	8946.90		8934.60	8.2E−25	9 [7]	5 [4]	14 [1]
(310)–(000)	9005.45	9005.50[b]	9005.35	1.6E−23	14 [7]	8 [3]	102 [10]
(211)–(000)	9050.34	9050.349	9050.36	2.7E−22	16 [13]	9 [6]	175 [99]
(112)–(000)	9202.50	9202.716	9201.90	1.4E−23	17	9	139
(013)–(000)	9366.04	9366.313	9365.45	4.0E−23	16	9	157
(221)–(010)	10180.04	10180.116		1.8E−25	7	2	8
Total							687 [110]

The values given in brackets in the last three columns correspond to the results of Ref. [2].
[a] Rovibrational term value of the $[J, K_a, K_c] = [000]$ rotational level.
[b] Extrapolated value (see text).

Table 3
Rovibrational term values (cm^{-1}) of the (211), (013), (112), and (310) vibrational states of D_2O

J	K_a	K_c	E_{obs}	σ	N	E_{obs}	σ	N	E_{obs}	σ	N	E_{obs}	σ	N
			(211)			(013)			(112)			(310)		
0	0	0	9050.3491		1	9366.3131		1	9202.7161		1			
1	0	1	9062.1269	0.1	2	9378.2183	0.9	3	9214.5253	0.4	2			
1	1	1	9070.4485	0.1	2	9385.8134	0.1	2	9222.6108	0.7	3			
1	1	0	9073.0026	0.1	2	9388.4329		1	9225.1880	4.2	2			
2	0	2	9085.1652	0.4	2	9401.4525	0.7	2	9237.6197	0.9	3			
2	1	2	9091.6001	0.3	3	9407.0114	0.5	3	9243.6639		1	9046.7648		1
2	1	1	9099.1830	0.1	3	9414.8626	0.1	2	9251.3841	0.5	2			
2	2	1	9123.9822	0.2	2	9437.5497	0.2	2	9275.5375	0.6	3			
2	2	0	9124.4854	0.5	2	9438.1178		1	9276.0602	0.1	3	9080.6049		1
3	0	3	9118.5536	0.1	2	9435.0281	0.1	2	9271.0653	0.9	3			
3	1	3	9123.3248	0.2	3	9438.4713	0.1	2	9274.9322	0.1	2	9077.8118		1
3	1	2	9138.0084	0.1	3	9454.0691	0.1	2	9290.2815	0.3	3			
3	2	2	9158.2296	0.1	4	9473.2958	0.1	3	9310.9979	0.5	3	9115.1924		1
3	2	1	9160.2255	0.3	3	9475.9695	0.1	3	9313.4759	2.5	2	9116.8798	0.4	3
3	3	1	9207.0890	0.1	2	9517.6213		1	9357.6145	0.1	2	9166.2796	0.2	3
3	3	0	9207.1534	0.1	2	9517.6986		1	9357.6846		1	9165.9343	0.1	2
4	0	4	9161.3976	0.8	3	9478.0494	0.1	2	9313.9844		1	9116.2677		1
4	1	4	9162.5168	0.1	3	9479.8975	0.1	3	9316.1233	1.5	2			
4	1	3	9188.9211	0.7	3	9505.4402	0.1	3	9341.3245	0.4	3			
4	2	3	9204.1342	0.3	3	9520.4683	0.1	2	9357.8349		1	9161.5286		1
4	2	2	9208.7318	0.1	2	9527.6437	0.2	3	9364.5408	0.8	2	9169.0727	0.2	2
4	3	2	9254.3510	0.1	3	9566.2800	0.5	3	9405.8246	2.8	2	9216.1242	0.3	3
4	3	1	9254.7773	0.3	3	9566.8169	1.5	2	9406.2818	0.6	3	9214.5633	3.3	3
4	4	1	9320.0584	1.2	2	9626.3267	2.1	2	9469.1468		1	9280.5139		1
4	4	0	9320.0564 B		1	9626.3302	7.1	2	9469.1504	1.1	2	9280.5034	1.2	2
5	0	5	9213.2453	0.1	2	9530.1276	1.8	3	9365.9420		1	9168.0988		1
5	1	5	9213.9897	0.1	3	9531.1261	0.8	2	9366.9997		1	9169.3919		1
5	1	4	9251.0985	0.2	2	9568.0513	0.1	2	9403.6777	1.0	2			
5	2	4	9261.4860	0.1	3	9578.6786	0.2	2	9415.6891	2.0	2	9218.8874	0.8	3
5	2	3	9279.4461	0.1	2	9593.0575	0.1	2	9429.2720		1	9232.1989		1
5	3	3	9313.5642	0.3	3	9627.1156	0.3	2	9466.1194	1.2	4	9269.3378	0.2	3
5	3	2	9315.1482	0.2	3	9629.1143	0.6	3	9467.8545	1.6	3	9275.4248	1.6	3
5	4	2	9379.3316	0.1	4	9687.3800	0.5	2	9529.5947	2.2	3	9340.8330	1.2	2
5	4	1	9379.4193	0.1	2	9687.4597	0.4	2	9529.5547		1	9340.8207		1
5	5	1	9462.3966		1	9763.2043	2.9	2	9609.6508	0.3	3	9425.9828		1
5	5	0	9462.3961		1	9763.2068	0.1	2	9609.6534		1	9425.9771		1
6	0	6	9274.0410	0.4	3	9591.2429	0.4	2	9426.9151		1	9228.8518		1
6	1	6	9274.3852	0.3	3	9591.6053	1.1	2	9427.3554		1	9229.4717		1
6	1	5	9323.5122	0.2	2	9640.7975	0.5	3	9476.2870	0.1	2	9277.8120		1
6	2	5	9329.8748	0.7	4	9647.5028	0.1	4	9484.1648	0.1	2	9286.8947	1.1	2
6	2	4	9356.1734	0.2	3	9671.5560	0.1	2	9507.1199	1.5	2	9309.0126		1
6	3	4	9384.6231	1.0	3	9699.9032	0.2	3	9538.3289	0.4	2	9341.4772	0.9	3
6	3	3	9388.8519	0.9	2	9705.2442	0.3	3	9543.0208	1.5	3	9349.1594	0.1	2
6	4	3	9450.6924	0.2	2	9760.8272	0.1	3	9602.6223	0.5	2	9413.5424		1
6	4	2	9451.0380	0.2	3	9761.2088	0.9	2	9602.9687	0.5	3	9413.5054	0.1	2
6	5	2	9533.5363	0.5	2	9836.6913	3.6	2	9682.4428		1	9498.5718		1
6	5	1	9533.5300	0.4	2	9836.6989	3.4	2	9682.4130	0.2	2	9498.5765		1
6	6	1	9633.3519		1	9927.5318	0.2	2	9778.3592	2.9	2	9597.9416		1
6	6	0	9633.3518		1	9927.5320	0.1	2	9778.3617	0.1	2	9597.9411		1
7	0	7	9343.8657	2.4	2	9661.4995	0.1	2	9496.3264	2.4	2	9298.5873	1.0	2
7	1	7	9344.0033		1	9661.6055		1	9497.0793		1	9298.8670		1
7	1	6	9405.2075	0.3	5	9722.7787	0.2	2	9558.2255	0.4	2			
7	2	6	9408.7053	0.3	3	9726.5272	1.2	2	9562.8797	1.7	2	9365.1559	2.1	2
7	2	5	9445.4502	0.5	3	9761.9855	0.4	3	9597.2098		1			
7	3	5	9467.3258	0.1	3	9784.3029	0.6	3	9622.1383	1.2	2	9424.9222	1.8	3
7	3	4	9476.1174	0.3	3	9795.5788	0.1	3	9632.2133		1	9436.4818	0.1	2
7	4	4	9534.1445	0.4	2	9846.6435	0.6	3	9688.0755	1.2	2	9497.9309	0.1	2
7	4	3	9535.2527	0.3	2	9847.9366	1.6	2	9689.0735	2.1	2	9499.1891	2.3	2
7	5	3	9616.8332		1	9922.5705	0.6	2	9767.6405	0.1	3	9583.5619 B		1
7	5	2	9616.7882	0.1	2	9922.6295	1.0	3	9767.3439		1			
7	6	2	9716.2008	0.1	2	10013.7992	0.8	3	9863.8034		1	9681.6444		1

Note: "B" and "T" denotes an energy level derived from a blended line and with tentative assignment, respectively (see text).

Table 3 (*continued*)

J	K_a	K_c	E_{obs}	σ	N	E_{obs}	σ	N	E_{obs}	σ	N	E_{obs}	σ	N
			(211)			(013)			(112)			(310)		
7	6	1	9716.2006	0.1	2	10013.7993	0.7	2	9863.8029		1			
7	7	1	9832.0890		1	10118.4636		1	9974.3863	1.2	2	9801.3239		1
7	7	0	9832.0896		1	10118.4637		1	9974.3864	1.4	2	9801.3238		1
8	0	8	9422.7354	0.1	2	9741.0051	0.3	2	9576.0025	0.4	2	9377.3749	1.1	2
8	1	8	9422.8304		1	9740.9440	0.2	2	9576.1511	0.7	2	9377.4965		1
8	1	7	9495.6623	0.2	2	9813.6350		1	9649.0638	3.5	2	9450.2332	2.0	2
8	2	7	9497.4044	0.1	2	9815.4151	1.2	3	9651.5067		1	9453.3218	1.0	2
8	2	6	9546.0868	0.7	2	9861.9395	1.6	3	9698.3389		1			
8	3	6	9561.3073	0.6	4	9879.8800	1.0	3	9717.1099	2.7	2			
8	3	5	9577.6590	0.5	2	9899.8743		1	9735.3275		1	9537.7266		1
8	4	5	9629.5719	0.2	3	9944.7026 B		1	9785.6992		1	9595.3181		1
8	4	4	9632.5266	1.5	2	9948.1522		1	9788.1512	0.1	2	9595.4145		1
8	5	4	9712.4989	0.1	3	10020.8560		1	9866.5187	0.1	2	9675.0124		1
8	5	3	9712.3182	0.9	2	10021.0917	0.4	2	9864.5083	0.1	2	9675.2442		1
8	6	3	9811.1374	0.5	2	10112.4398	0.1	2	9961.2333 B	5.8	2			
8	6	2	9811.1372		1	10112.4378	2.1	2	9961.2034	1.6	2	9777.7965		1
8	7	2	9926.4057	0.2	2	10218.7196		1	10074.2845	4.2	2	9898.0059		1
8	7	1	9926.4055	0.2	2	10218.7193		1	10074.2866	2.0	2	9898.0055		1
8	8	1	10056.8914		1	10335.1032		1	10196.2738		1			
8	8	0	10056.8915		1	10335.1033		1	10196.2741		1			
9	0	9	9510.7961	0.7	2	9830.3993		1	9662.4071	0.8	4	9465.2445		1
9	1	9	9510.8264		1	9829.7153		1	9665.2776	0.7	2	9465.2930		1
9	1	8	9594.8078	0.3	2	9913.5461	1.0	2	9749.0735	2.9	2			
9	2	8	9595.6180	0.1	2	9913.9233	0.2	2	9749.8323		1	9551.0989		1
9	2	7	9656.1392		1	9978.2694		1	9809.0222		1			
9	3	7	9668.5840	0.1	2	9986.1738	0.1	2	9822.2300	2.4	4	9624.6888	2.8	2
9	3	6	9690.4669	0.7	3	10017.3094	0.2	2	9851.6868		1	9652.5353		1
9	4	6	9736.4897	0.9	2	10054.7249		1	9895.0698	2.8	4	9707.2929	0.2	2
9	4	5	9743.3842	0.3	3	10062.4006	0.8	2	9901.1331	0.6	2	9707.4509		1
9	5	5	9820.7478	0.1	2	10131.5143		1	9971.0345	2.6	3	9784.3961		1
9	5	4	9820.2921	0.5	2	10132.2593	0.5	3	9974.0199		1	9784.9530		1
9	6	4	9918.2480	1.4	2	10223.4185	0.1	2	10070.6824	0.1	2			
9	6	3	9918.2114	0.4	2	10223.4529		1	10070.6292	1.2	2			
9	7	3	10032.8708	0.5	2	10332.1106		1	10184.7204	3.8	2	10006.8093		1
9	7	2	10032.8707	0.9	2	10332.1109		1	10184.7304	5.8	2	10006.8051		1
9	8	2	10162.0657	0.4	2	10438.5545		1	10299.8881		1			
9	8	1	10162.0654	0.2	2	10438.5541		1	10299.8885		1			
9	9	1	10319.8470		1	10576.5308 T		1						
9	9	0	10319.8470		1	10576.5308 T		1						
10	0	10	9607.9739		1	9926.3652	1.0	2	9761.0745	0.5	2			
10	1	10	9607.9890	4.3	2	9925.0682	0.2	3	9760.7071	1.5	3	9562.2482		1
10	1	9	9702.7539		1	10024.0376	0.6	2	9852.1616	0.6	2	9657.8962		1
10	2	9	9703.1783		1	10021.9675	0.7	2	9857.9699		1	9658.3011	11.0	2
10	2	8	9778.2810		1	10090.7803	0.4	2	9931.0272	0.3	2			
10	3	8	9783.5173	0.3	3	10102.7588	0.1	2	9940.4828	2.0	3	9740.2731	0.8	2
10	3	7	9831.0789		1	10146.6944	7.9	2	9980.2311		1	9780.0929		1
10	4	7	9860.8982	1.9	2	10176.3631	0.7	3	10014.8335	2.3	2	9814.0393		1
10	4	6	9868.1198		1	10190.9300	1.3	2	10027.7673	3.7	2			
10	5	6	9941.6670	0.3	2	10254.4255	1.6	2	10100.3412		1	9905.4452		1
10	5	5	9941.0064	0.3	3	10256.3869	1.6	2	10096.1233		1	9906.6481		1
10	6	5	10037.6247	0.7	2	10346.7080	0.2	2	10192.2891		1			
10	6	4	10037.5239	0.1	2	10346.8331		1	10192.0971	0.2	2	10006.5790		1
10	7	4	10151.4986		1							10127.7417		1
10	7	3	10151.5634		1							10127.7221		1
10	8	3	10279.8491		1	10556.5753		1	10417.1168		1			
10	8	2	10279.8492		1	10556.5748		1	10417.1190		1			
10	9	2	10441.3162 T		1				10579.6649 T		1			
10	9	1	10441.3140 T		1				10579.6645 T		1			
11	0	11	9714.2630 B		1	10033.5529	0.5	3				9668.2602		1
11	1	11	9714.2872 B		1	10033.5675	9.2	2	9868.3353		1	9668.2831		1
11	1	10	9819.6446	1.4	2	10133.5175		1				9774.1409		1
11	2	10	9819.7981	0.7	2	10139.9244		1	9978.2241	0.8	2	9774.7241		1
11	2	9	9906.7247	0.3	2	10220.5129	5.1	2						

(*continued on next page*)

Table 3 (*continued*)

J	K_a	K_c	E_{obs}	σ	N	E_{obs}	σ	N	E_{obs}	σ	N	E_{obs}	σ	N
			(211)			(013)			(112)			(310)		
11	3	9	9909.6860	0.4	2	10229.3137	1.4	2	10066.9301	0.3	2			
11	3	8	9965.0596		1	10287.0707	0.6	2						
11	4	8	9989.3828		1	10309.1801	0.3	2	10152.6441		1	9947.9060 B	9.7	2
11	4	7	10006.3260	1.0	2	10333.3999	1.6	2	10168.2125		1	9970.2381		1
11	5	7	10074.0624	0.6	2	10389.3402		1	10232.8107		1	10038.3314	2.7	2
11	5	6	10074.8535	0.6	3	10393.3823		1						
11	6	6	10169.3910	1.2	2				10326.1487	4.1	2	10139.0419		1
11	6	5	10169.1552	1.2	2	10482.6111 T		1						
11	7	5				10594.1603		1						
11	7	4	10282.1321		1	10594.1625		1						
11	8	4	10410.0137	1.2	2							10396.1731		1
11	8	3	10410.0132	0.9	2									
12	0	12	9829.9692		1	10149.8397	5.7	2	9983.3622		1	9783.4491		1
12	1	12	9828.9798		1	10149.8462	1.6	2	9982.9097		1			
12	1	11	9945.5708		1	10263.1687	1.2	2	10098.4040	0.5	3			
12	2	11	9945.7548	1.0	2	10261.1554		1	10097.5096 T		1	9900.1132		1
12	2	10	10043.8656	0.3	2	10359.0473		1						
12	3	10	10046.4020	0.2	2	10365.7124		1				10001.5253		1
12	3	9	10120.5471		1				10273.9478		1			
12	4	9				10452.7380		1						
12	4	8	10156.4390	0.7	2	10488.9450		1						
12	5	8	10217.9891		1	10535.8544		1				10182.2374		1
12	5	7	10222.2962		1	10546.2561		1						
12	6	7	10313.6307		1	10629.9348		1						
12	7	5	10425.1681		1							10406.1659		1
13	0	13	9954.0170		1	10275.1751		1	10107.6836	0.6	2	9907.8044		1
13	1	13	9954.0217		1	10275.1798		1	10107.6810	1.3	2			
13	1	12	10080.7793		1	10399.1967		1				10034.7933		1
13	2	12	10079.8562		1	10398.9075		1	10231.4854 T		1			
13	2	11	10189.6501	1.0	2	10505.9316		1						
13	3	11	10189.0473 B		1	10512.5587		1	10355.4614		1			
13	3	10	10277.6992		1	10594.4715		1						
13	4	10	10283.3145		1	10606.6861		1				10239.6800		1
13	4	9				10656.3424		1						
13	5	9										10323.7000 T		1
13	5	8	10383.6034		1									
13	6	7	10469.9740		1									
14	0	14	10087.6493		1	10409.6433 B		1	10241.5757		1	10040.7687		1
14	1	14	10087.6517		1	10409.6457 B		1	10241.5755		1			
14	1	13	10223.9922		1							10178.7675		1
14	2	13	10224.1543	4.4	2									
14	2	12	10344.3774		1									
14	3	12	10343.6529		1	10674.8984		1						
14	4	11	10446.2183		1	10770.9180		1						
14	5	10	10540.2599		1									
14	5	9	10558.6213		1									
14	6	9	10638.8918		1									
15	0	15	10230.6034		1				10384.5040		1			
15	1	15	10230.6040		1				10384.5034		1			
15	1	14	10377.1852		1	10697.8060		1						
15	2	14	10377.2306		1	10697.7710		1						
15	6	9	10822.3077 T		1									
16	0	16	10381.8417		1	10705.8909		1	10536.4783		1			
16	1	16	10381.8805		1	10705.8911		1	10536.4781		1			
16	1	15	10538.5269 T		1									
17	0	17							10697.4908		1			
17	1	17							10697.4916		1			

region has been assigned on the basis of high quality variational calculations. The combination of these two high sensitive absorption spectra recorded independently with different experimental conditions has allowed for the determination of a precise and extensive set of 577 new rotational energy levels belonging to eight vibrational states: (211), (013), (112), (310), (032), (230), and (131). Intensity measurements were also performed and integrated intensi-

Table 4
Rovibrational term value (cm^{-1}) of the (131), (230), (032), and (221) vibrational states of D_2O

J	K_a	K_c	E_{obs}	σ	N
(131)					
2	0	2	8827.9372		1
2	1	2	8836.9636		1
2	2	1	8878.9672		1
2	2	0	8879.4227		1
3	1	3	8868.3267		1
3	1	2	8884.9717		1
3	2	2	8915.0652		1
3	2	1	8917.2036	1.1	2
3	3	0	8977.1352		1
4	0	4	8905.5603		1
4	1	4	8909.7296		1
4	2	3	8962.8056		1
4	2	2	8968.6423		1
4	3	2	9024.9379	0.3	2
4	3	1	9025.2562		1
4	4	1	9109.8641		1
4	4	0	9109.8584		1
5	0	5	8958.2323		1
5	1	5	8961.2281		1
5	1	4	9001.0199		1
5	2	4	9021.9902		1
5	2	3	9033.9278		1
5	3	2	9086.0735	1.5	2
5	4	2	9170.1807	2.1	2
5	4	1	9170.1886	0.1	2
5	5	1	9275.7547		1
5	5	0	9275.7542		1
6	1	6	9020.6032		1
6	1	5	9075.7559		1
6	2	4	9112.8062		1
6	3	4	9156.9311		1
6	3	3	9160.0166		1
6	4	3	9242.7916		1
6	5	2	9348.1171		1
6	5	1	9348.1114		1
7	0	7	9090.1588		1
7	1	7	9090.8145		1
7	1	6	9160.2931		1
7	2	6	9166.3766		1
7	2	5	9204.6181		1
7	3	4	9247.2419		1
7	4	3	9328.0398		1
7	5	3	9432.7100		1
7	5	2	9432.7157		1
7	7	1	9704.6349		1
7	7	0	9704.6350		1
8	0	8	9169.5456		1
8	1	8	9170.0739		1
8	1	7	9253.8065		1
8	2	6	9308.3723		1
8	3	6	9337.2220		1
8	4	5	9424.9408	0.9	2
8	5	4	9529.6289		1
8	6	3	9653.0110		1
8	6	2	9653.0114		1
8	7	2	9804.5583		1
8	7	1	9804.5580		1
8	8	1	9957.7204		1
8	8	0	9957.7205		1
9	2	7	9424.3487		1
9	3	7	9444.4840 T		1
9	3	6	9476.2658		1
9	4	5	9537.4163		1
9	5	4	9638.9859		1
9	6	4	9761.7077 B		1
9	6	3	9761.7119 B		1
9	9	1	10238.1021		1
9	9	0	10238.1021		1
10	1	10	9355.1398		1
10	2	9	9467.9698 T		1
10	2	8	9548.9390 T		1
10	3	8	9563.3843		1
10	5	6	9760.4473	0.5	2
10	9	2	10361.0684		1
10	9	1	10361.0693		1
11	6	6	10016.3832 T		1
11	6	5	10016.4522		1
12	2	10	9825.0200		1
12	3	10	9831.8894	0.8	2
12	5	8	10039.6922		1
13	6	7	10316.4475		1
(230)					
4	3	1	8949.7629		1
5	2	4	8941.6844		1
6	3	3	9082.8504		1
6	6	0	9412.9272 B		1
7	4	4	9260.9934		1
7	6	2	9498.8748		1
7	6	1	9498.1977		1
8	6	3	9596.6980		1
8	6	2	9596.7881		1
9	6	4	9705.3255		1
10	5	5	9697.6274	1.3	2
(032)					
4	4	1	9255.7542		1
4	4	0	9255.7593		1
5	4	2	9317.3158		1
5	5	1	9416.7155		1
5	5	0	9416.7098		1
6	4	3	9391.2887		1
7	4	4	9477.7838	0.7	2
7	5	3	9577.1621		1
7	5	2	9577.2365		1
8	4	5	9575.6110	0.1	2
8	5	4	9681.3446		1
8	5	3	9681.4500		1
9	4	6	9686.2850		1
9	5	4	9792.2592		1
(221)					
1	0	1	10191.9183		1
1	1	0	10204.0985		1
2	1	2	10222.6557		1
2	2	1	10258.7775		1
3	0	3	10248.4661		1
4	0	4	10291.3992		1
4	1	4	10293.6265		1
7	1	6	10538.9828		1

Note. N is the number of lines used for the upper energy level determination and σ denotes the corresponding experimental uncertainty in 10^{-3} cm^{-1} units. "B" denotes the energy level derived from blended line and then with an accuracy worse than the averaged one. Energy levels marked with "T" were derived from lines with tentative assignment (see text).

ties of the considered vibrational bands were estimated. The comparison of two variational calculations: Partridge and Schwenke (PES of Ref. [24] and DMS of Ref. [21]) and that obtained by combining the PES of Ref. [20] with the DMS of Ref. [21], has shown that the PS calculation starts to diverge at $J \geqslant 10$, leading to irregular (obs. − calc.) deviations as large as $1.53\ \mathrm{cm}^{-1}$, while the new one shows regular and smooth (obs. − calc.) tendencies up to $J = 17$. However, these new calculations deviate from the experimental rovibrational term value by up to $0.4\ \mathrm{cm}^{-1}$, which may in certain cases prevent performing unambiguous assignment. The experimental data derived in this paper by combining ICLAS-VeCSEL and FTS spectra will help to further refine both the PES and the DMS of the D_2O molecule.

Acknowledgments

This work, performed in the frame of the European research network QUASAAR (MRTN-CT-2004-512202), is jointly supported by the INTAS foundation (Project 03-51-3394) as well as a collaborative project between CNRS and RFBR (PICS Grant No. 05-05-22001) and the Russian Foundation for Basic Research (06-02-16082-a). It takes part in an effort by a Task Group of the International Union of Pure and Applied Chemistry (IUPAC, Project No. 2004-035-1-100) to compile, determine, and validate, both experimentally and theoretically, accurate frequency, energy level, line intensity, line width, and pressure effect spectral parameters of all major isotopologues of water. AJ (Reims) and AC (Grenoble) are grateful for the financial support provided by Programme national de Chimie de l'Atmosphère SF and ACV (Brussels) also thank the Belgian Federal Science Policy Office (Contract EV/11/03C), the Fonds National de la Recherche Scientifique (FNRS, Belgium) and the European Space Agency (ESA-Prodex program). Authors are indebted to Sergei Tashkun for providing them with the D_2O synthetic linelist based on the PES and DMS calculated by Partridge and Schwenke.

Appendix A. Supplementary data

Supplementary data for this article are available on ScienceDirect (www.sciencedirect.com) and as part of the Ohio State University Molecular Spectroscopy Archives (http://msa.lib.ohio-state.edu/jmsa_hp.htm).

References

[1] A.D. Bykov, V.P. Lopasov, Yu.S. Makushkin, L.N. Sinitsa, O.N. Ulenikov, V.E. Zuev, J. Mol. Spectrosc. 94 (1982) 1–27.
[2] Jing-Jing Zheng, O.N. Ulenikov, G.A. Onopenko, E.S. Bekhtereva, Sheng-Gui He, Xiang-Huai Wang, Shui-Ming Hu, Hai Lin, Qing-Shi Zhu, Mol. Phys. 99 (2001) 931–937.
[3] O.N. Ulenikov, Shui-Ming Hu, E.S. Bekhtereva, G.A. Onopenko, Sheng-Gui He, Xiang-Huai Wang, Jing-Jing Zheng, Qing-Shi Zhu, J. Mol. Spectrosc. 210 (2001) 18–27.
[4] Shui-Ming Hu, O.N. Ulenikov, E.S. Bekhtereva, G.A. Onopenko, Sheng-Gui He, Hai Lin, Ji-Xin Cheng, Qing-Shi Zhu, J. Mol. Spectrosc. 212 (2002) 89–95.
[5] O.N. Ulenikov, Sheng-Gui He, G.A. Onopenko, E.S. Bekhtereva, Xiang-Huai Wang, Shui-Ming Hu, Hai Lin, Qing-Shi Zhu, J. Mol. Spectrosc. 204 (2000) 216–225.
[6] O. Naumenko, O. Leshchishina, A. Campargue, J. Mol. Spectrosc. 236 (2006) 58–69.
[7] P.-F. Coheur, S. Fally, M. Carleer, C. Clerbaux, R. Colin, A. Jenouvrier, M.-F. Mérienne, C. Hermans, A.C. Vandaele, J. Quant. Spectrosc. Radiat. Transfer 74 (2002) 493–510.
[8] S. Fally, P.-F. Coheur, M. Carleer, C. Clerbaux, R. Colin, A. Jenouvrier, M.-F. Mérienne, C. Hermans, A.C. Vandaele, J. Quant. Spectrosc. Radiat. Transfer 82 (2003) 119–132.
[9] M.-F. Mérienne, A. Jenouvrier, M. Carleer, P.-F. Coheur, R. Colin, S. Fally, C. Hermans, A.C. Vandaele, M. Bach, J. Quant. Spectrosc. Radiat. Transfer 89 (2003) 99–118.
[10] F.O. Libnau, A.A. Christy, O.M. Kvalheim, Appl. Spectrosc. 49 (1995) 1431–1437.
[11] M. Bach, S. Fally, P.-F. Coheur, M. Carleer, A. Jenouvrier, A.C. Vandaele, J. Mol. Spectrosc. 232 (2005) 341–350.
[12] A. Garnache, A.A. Kachanov, F. Stoeckel, R. Houdré, J. Opt. Soc. Am. B 17 (2000) 1589–1598.
[13] E. Bertseva, A.A. Kachanov, A. Campargue, Chem. Phys. Lett. 351 (2002) 18–26.
[14] Y. Ding, V.I. Perevalov, S.A. Tashkun, J.-L. Teffo, S. Hu, E. Bertseva, A. Campargue, J. Mol. Spectrosc. 220 (2003) 80–86.
[15] E. Bertseva, V. Perevalov, S.A. Tashkun, A. Campargue, J. Mol. Spectrosc. 226 (2004) 196–200.
[16] O. Naumenko, A. Campargue, J. Mol. Spectrosc. 221 (2003) 221–226.
[17] O.N. Ulenikov, S.-M. Hu, E.S. Bekhtereva, Q.-S. Zhu, J. Mol. Spectrosc. 231 (2005) 57–65.
[18] L.S. Rothman, D. Jacquemart, A. Barbe, D. Chris Benner, M. Birk, L.R. Brown, M.R. Carleer, C. Chackerian Jr., K. Chance, V. Dana, V.M. Devi, J.-M. Flaud, R.R. Gamache, A. Goldman, J.-M. Hartmann, K.W. Jucks, A.G. Maki, J.Y. Mandin, S.T. Massie, J. Orphal, A. Perrin, C.P. Rinsland, M.A.H. Smith, J. Tennyson, R.N. Tolchenov, R.A. Toth, J. Vander Auwera, P. Varanasi, G. Wagner, J. Quant. Spectrosc. Radiat. Transfer. Journal of Quantitative Spectroscopy & Radiative Transfer 96 (2005) 139–204.
[19] E. Bertseva, A. Campargue, Opt. Commun. 232 (2004) 251–261.
[20] S.V. Shirin, N.F. Zobov, O.L. Polyansky, J. Tennyson, T. Parekunnel, P.F. Bernath, J. Chem. Phys. 120 (2004) 206–210.
[21] D.W. Schwenke, H. Partridge, J. Chem. Phys. 113 (2000) 6592–6597.
[22] O.L. Polyansky, A.G. Csaszar, S.V. Shirin, N.F. Zobov, P. Barletta, J. Tennyson, D.W. Schwenke, P.J. Knowles, Science 299 (2003) 539–542.
[23] J. Tennyson, M.A. Kostin, P. Barletta, G.J. Harris, J. Ramanlal, O.L. Polyansky, N.F. Zobov, Comp. Phys. Commun. 163 (2004) 85–116.
[24] H. Partridge, D.W. Schwenke, J. Chem. Phys. 106 (1997) 4618–4639.
[25] S.N. Mikhailenko, G.Ch. Mellau, E.N. Starikova, S.A. Tashkun, Vl.G. Tyuterev, J. Mol. Spectrosc. 233 (2005) 32–59.
[26] G.Ch. Mellau, S.N. Mikhailenko, E.N. Starikova, S.A. Tashkun, H. Over, Vl.G. Tyuterev, J. Mol. Spectrosc. 224 (2004) 32–60.
[27] A. Bykov, O. Naumenko, L. Sinitsa, B. Voronin, J.-M. Flaud, C. Camy-Peyret, R. Lanquetin, J. Mol. Spectrosc. 205 (2001) 1–8.
[28] O.N. Ulenikov, Sheng-Gui He, G.A. Onopenko, E.S. Bekhtereva, Xiang-Huai Wang, Shui-Ming Hu, Hai Lin, Qing-Shi Zhu, J. Mol. Spectrosc. 204 (2000) 216–225.